

SUPER Decoder Block for Reconstruction-Aware U-Net Variants

Siheon Joo¹, and Hongjo Kim^{2*}

¹Integrated M.S./Ph.D. Student, Dept. of Civil and Environmental Engineering, Yonsei Univ., Seoul, Korea.

²*Assistant Professor, Dept. of Civil and Environmental Engineering, Yonsei Univ., Seoul, Korea.

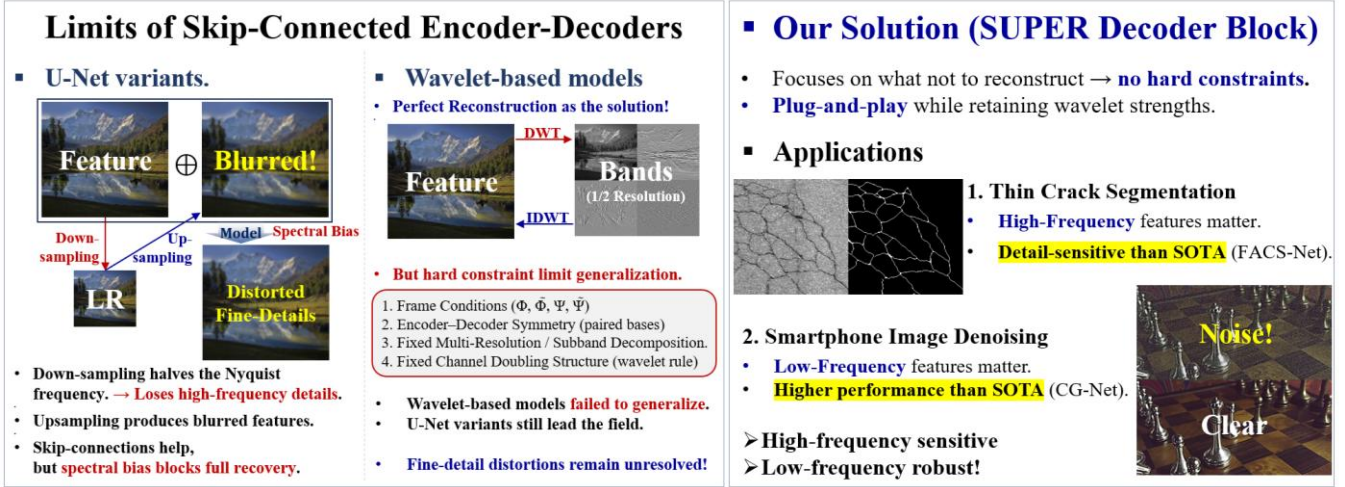


Figure 1. SUPER Decoder Block: A plug-and-play unit that brings wavelet-like reconstruction & frequency awareness to U-Net variants.

Abstract

Skip-connected encoder-decoder architectures (U-Net variants) are widely adopted for inverse problems but still suffer from information loss, limiting recovery of fine high-frequency details. We present **Selectively Suppressed Perfect Reconstruction (SUPER)**, which exploits the perfect reconstruction (PR) property of wavelets to prevent information degradation while selectively suppressing (SS) redundant features. Free from rigid framelet constraints, SUPER serves as a plug-and-play decoder block for diverse U-Net variants, eliminating their intrinsic reconstruction bottlenecks and enhancing representational richness. Experiments across diverse crack benchmarks, including state-of-the-art (SOTA) models, demonstrate the structural potential of the proposed SUPER Decoder Block. Maintaining comparable computational cost, SUPER enriches representational diversity through increased parameterization. In small-scale in-domain experiments on the CrackVision12K dataset, SUPER markedly improves thin-crack segmentation performance, particularly for cracks narrower than 4 px, underscoring its advantage in high-frequency-dominant settings. In smartphone image denoising on SIDD, where low-frequency components prevail, SUPER still achieves a moderate gain in PSNR, confirming its robustness across low- and high-frequency regimes. These results validate its plug-and-play generality across U-Net variants, achieving high-frequency fidelity and global coherence within a unified, reconstruction-aware framework.

1. Introduction

With the rapid advances in deep learning for computer vision, tasks that require precise recovery of fine details—such as local anomalies or subtle texture patterns—have become increasingly important [1], [2]. Such fine-scale structures are typically high-frequency or spectrally sparse, and they are easily lost in conventional encoder-decoder architectures because downsampling and convolution tend to attenuate or distort high-frequency information [3]. Among various approaches, skip-connected encoder-decoder architectures (e.g., the U-Net variants [4]) have become the most widely adopted solution [5]. Yet, they still face fundamental challenges in recovering such fine details. Specifically, during decoding, coarse global features must be upsampled—an ill-posed operation that inevitably distorts high-frequency content [6], [7]. While skip connections partially reintroduce spatial details from earlier layers [8], truly high-frequency signals remain sparse and insufficient [9]. Compounding this issue, deep neural networks exhibit a spectral bias, favoring low-frequency patterns while neglecting fine details [10], [11].

One promising direction to address these issues is to leverage wavelet transforms within the network [3]. The discrete wavelet transform (DWT) provides a downsampling operation that is **perfectly invertible** [3], minimizing information loss [6], [12], and it explicitly separates features into frequency bands [13], which can help counteract spectral bias [14]. Wavelet-based CNNs have shown high potential for preserving details [3], [15],

[16]. However, these architectures are typically complex and inflexible—often constrained by strict structural conditions such as tight-frame constraints [3], where the encoder and decoder must form energy-preserving dual filter banks. Such constraints enforce fixed analysis–synthesis relationships and rigid sampling structures, limiting architectural flexibility and hindering generalization across diverse tasks [17]. Furthermore, because high-frequency signals are inherently sparse and standard evaluation metrics emphasize average performance, improvements in fine-detail reconstruction may not significantly boost overall scores [18]. As a result, conventional U-Net variants architectures remain dominant despite their weaknesses [19], [20], [21].

Nevertheless, high-frequency distortions can severely degrade fine-detail accuracy, even when aggregate metrics remain unaffected [22]. For example, a model that blurs out high-frequency content will fail to detect the thinnest cracks in segmentation tasks [23], [24], miss micro-lesions in medical imaging [25], or produce artifacts in denoising and diffusion applications [26], regardless of high average accuracy on coarser structures. Conversely, high-frequency-biased architectures often amplify noise and destabilize low-frequency reconstruction, underscoring the challenge of spectral balance [14], [22]. Despite its broad importance, the preservation of high-frequency details remains often overlooked [27]. We thus aim for a broadly applicable decoder that mitigates U-Net variant’s detail loss.

In this paper, we propose the **Selectively Suppressed Perfect Reconstruction (SUPER) Decoder Block**—a plug-in decoder-stage block for U-Net variants that incorporates the benefits of wavelet-based designs. Inspired by the conditional perfect reconstruction (PR) property of wavelet transforms [3], SUPER selectively suppresses redundant features while retaining task-relevant high-frequency details. Free from tight frame constraints, it flexibly adapts to various encoder–decoder architectures. Evaluations on state-of-the-art (SOTA) backbones—including **FACS-Net** [28] for thin-crack segmentation, where high-frequency precision is critical, **CascadedGaze-Net** [29] for denoising, dominated by low-frequency reconstruction—demonstrate that SUPER consistently enhances structural fidelity across both spectral extremes, revealing its versatility and optimization challenges.

Key Contributions:

- We propose Selectively Suppressed Perfect Reconstruction (SUPER), a relaxed reconstruction framework that generalizes classical PR.
- We show that SUPER structurally resolves key reconstruction limits in U-Net variants, leading to more reliable high- and low-frequency recovery.

2. Related Works

2.1. Importance of Details in Inverse Problem

Fine-scale structures such as edges, textures, and thin lines critically influence perceptual realism and task-

specific accuracy across domains yet remain challenging to preserve. Prior surveys in video super-resolution [1] and high-resolution image processing [2] highlight that even minor structural degradations can degrade interpretability, a problem echoed in crack detection [23], [24], medical imaging [25], and acoustic tomography denoising [26]. Recent works address these issues through frequency-aware losses (e.g., FFL [18]) and topology-aware constraints such as the Crack Topology Loss introduced in FACS-Net [28], which capture subtle distortions often overlooked by average-based metrics [30]. Collectively, these studies reveal both the necessity of high-frequency preservation and the inadequacy of current architectures to guarantee it.

2.2. Limitations of U-Net Variants

Skip-connected encoder–decoder networks, most notably the U-Net variants, remain the dominant design for detail-sensitive tasks due to their simplicity and strong feature reuse [5]. However, their decoders face intrinsic challenges that limit fine-detail recovery. First, the upsampling process inevitably discards structural information, producing blurred or distorted reconstructions even with skip connections [4], [8], [31], [32], [33]. Second, while skip connections reinject high-frequency cues, the transmitted details are typically sparse and low-energy, as reported in prior analyses of U-Net decoders [23], [25]. Third, neural networks exhibit spectral bias [10], preferentially fitting low-frequency components while underfitting high-frequency signals, which exacerbates the difficulty of recovering subtle textures [9], [11]. Fourth, many U-Net variants reduce costs by projecting fused features into fewer channels, but such compression risks discarding fine details [34], [35]. Collectively, these factors reveal that while U-Net variants architectures are widely adopted, they remain fundamentally constrained in reconstructing high-frequency details.

2.3. Wavelet-Based Architectures

Wavelet-integrated networks have emerged as promising alternatives for fine-detail preservation. By exploiting the perfect reconstruction property of wavelet transforms [3], they prevent information loss during sampling [6], [12] and explicitly separate features into frequency bands [36], enabling effective mitigation of spectral bias and facilitating frequency-aware operations [14], [37]. Such designs demonstrate strong capability in recovering subtle textures and thin structures across restoration and segmentation tasks [15], [16]. However, their applicability is hindered by rigid structural requirements, including fixed bases, symmetry or tight-frame constraints, and high integration cost [3], [17]. As a result, while wavelet-based architectures excel at preserving high-frequency details, their constrained design limits their role as a universal decoder.

2.4. Problem Statement

Building on the limitations outlined above, a fundamental mismatch emerges between practical decoder architectures and those that preserve high-frequency structure. This contrast highlights a dual gap: architectures in practice lack fine-detail fidelity, while architectures with such fidelity lack ease of integration. Bridging these gaps calls for a decoder design that can inherit the precision of wavelet methods while retaining the simplicity and flexibility required for seamless integration into existing encoder-decoder pipelines.

3. Theoretical Foundation

Deep Convolutional Framelets (DCF) [3] interpret encoder-decoder networks as paired frame operators $\Phi: \mathbb{R}^n \rightarrow \mathbb{R}^m$ and $\Psi: \mathbb{R}^m \rightarrow \mathbb{R}^n$ that ideally satisfy the perfect reconstruction (PR) condition:

$$\Psi\Phi = I,$$

ensuring distortion-free recovery under tight-frame constraints. Modern encoder-decoder architectures, however, rarely preserve such orthogonality or symmetric sampling, making strict PR neither realistic nor necessary.

For reconstruction-oriented tasks, the objective is not to reproduce the full input x but only the task-relevant component $x_{\mathcal{T}}$. We decompose the signal into orthogonal subspaces:

$$x = x_{\mathcal{T}} + x_{\mathcal{S}}, \quad \langle x_{\mathcal{T}}, x_{\mathcal{S}} \rangle = 0,$$

where \mathcal{T} contains informative content and $\mathcal{S} := \mathcal{T}^\perp$ denotes redundant or nuisance directions. This motivates relaxing PR into a *Conditional Perfect Reconstruction* (CPR) condition:

$$\Psi\Phi x = \mathcal{P}_{\mathcal{T}} x,$$

where $\mathcal{P}_{\mathcal{T}}$ is the orthogonal projection onto \mathcal{T} .

Although CPR provides a task-conditioned relaxation of strict perfect reconstruction, it does not specify how redundant components should be controlled within practical encoder-decoder architectures. Modern U-Net-like decoders lack explicit mechanisms for suppressing nuisance directions, which tend to propagate through upsampling layers and skip connections. Therefore, to operationalize CPR within real-world reconstruction networks, we introduce a learnable suppression operator that selectively contracts redundant subspaces while ensuring bounded deviations on task-relevant components.

To explicitly model selective reconstruction, we introduce the *Selectively Suppressed Perfect Reconstruction* (SUPER) operator:

$$\Psi\Phi = I - \mathcal{S}, \quad \|\mathcal{S}\| \leq \epsilon,$$

where \mathcal{S} is a learnable suppression operator acting on redundant components and ϵ bounds the allowable deviation from strict PR. Under this formulation, the reconstruction satisfies

$$\Psi\Phi x = x - \mathcal{S}(x), \quad \|\mathcal{S}(x)\|_2 \leq \epsilon \|x_{\mathcal{S}}\|_2,$$

ensuring a bounded and stable deviation from strict PR while suppressing redundant components.

To ensure that the suppression operator remains well-behaved, we impose a mild boundedness condition on its operator norm:

$$\|\mathcal{S}\|_2 \leq \epsilon < 1,$$

which guarantees that \mathcal{S} acts as a contraction on the redundant subspace $\mathcal{S} = \mathcal{T}^\perp$. This formalizes the bounded suppression assumption and ensures that nuisance components cannot be amplified.

Since each decoding stage satisfies $\|I - \mathcal{S}_k\|_2 \leq 1 + \epsilon$, the multi-stage SUPER decoder is a composition of uniformly bounded operators. Consequently, the overall reconstruction operator obeys

$$\|\Psi\Phi\|_2 \leq (1 + \epsilon)^L,$$

where L is the number of decoding stages. This upper bound prevents stage-wise error accumulation and ensures global stability of the full reconstruction process.

The strict PR case is recovered when the wavelet transform employs an orthonormal basis with symmetric boundary extension and when the fusion path preserves an identity connection. Under these conditions, $W^\top W = I$ and $\mathcal{S} = 0$, yielding $\Psi\Phi = I$.

Overall, SUPER generalizes DCF by replacing tight-frame PR with a bounded, task-conditioned reconstruction operator. This reconstruction-aware design is theoretically grounded and empirically validated, surpassing two state-of-the-art decoders on both HF- and LF-dominant benchmarks and demonstrating that a single, architecture-agnostic block can outperform specialized designs across contrasting spectral regimes.

4. Proposed Method

We present the **SUPER Decoder Block**, which modularizes the SUPER. By embedding selective suppression into the encoding-decoding process, the block preserves reconstruction-aware benefits while remaining plug-and-play for U-Net variants. An overview of the proposed block is illustrated in Figure 2.

4.1. Structural Formulation of SUPER

To embed the SUPER Decoder Block into existing architectures, we first generalize U-Net variants into a unified formulation. This abstraction provides a consistent basis for integrating SUPER within diverse encoder-decoder designs.

Generalization of U-Net Variants. Skip-connected encoder-decoder architectures, commonly referred to as the U-Net variants, can be abstracted into a unified formulation regardless of their implementation details. At each encoder stage k , features are transformed by $F_e^k(\cdot)$ (e.g., convolutional, residual, or transformer blocks) and then downsampled by $\mathcal{D}(\cdot)$:

$$x_e^k = \mathcal{D}(F_e^k(x_e^{k-1})). \quad (1)$$

In the decoder, resolution is progressively restored. The skip feature x_e^k is fused with the upsampled output of the deeper stage x_d^{k+1} :

$$x_d^k = F_d^k(x_e^k \oplus U(x_d^{k+1})), \quad (2)$$

Selected Suppressed Perfect Reconstruction (SUPER)

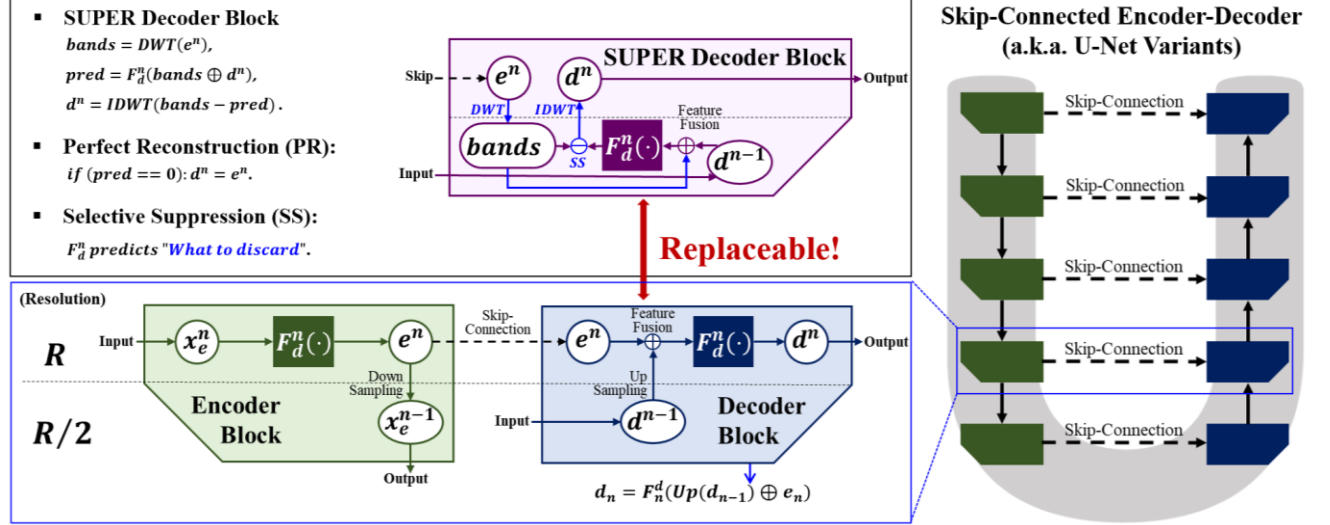


Figure 2. Structure of the proposed SUPER Decoder Block within generalized U-Net variants. The SUPER decoder block can replace conventional blocks by embedding wavelet-domain decomposition and selective suppression while preserving conditional perfect reconstruction.

where $\mathcal{U}(\cdot)$ denotes an upsampling operator (e.g., interpolation or transposed convolution), and \oplus is a fusion operator such as concatenation or element-wise sum. The decoder transformation F_d^k can adopt diverse forms, ranging from simple convolutions to transformer blocks. This abstraction captures the common principle of U-Net architectures—progressively compressing features in the encoder and reconstructing them in the decoder via skip connections—while implementation details differ across models.

Formulation of SUPER. Building upon the generalized U-Net formulation, our proposed SUPER can be regarded as a principled redesign of the decoder stage. Unlike conventional decoders that fuse skip features and upsampled activations only in the spatial domain, SUPER performs wavelet-domain decomposition and directly aligns the spatial resolution of the skip feature x_e^k and the deeper feature x_d^{k+1} through the discrete wavelet transform (DWT). This allows the low-frequency (LL) subband to support direct summation or concatenation with x_d^{k+1} without upsampling.

At decoder stage k , the SUPER is defined as:

$$x_d^k = W^\top (W(x_e^k) - F_d^k(W(x_e^k) \oplus x_d^{k+1})), \quad (3)$$

where $W(\cdot)$ and $W^\top(\cdot)$ denote the DWT and inverse DWT (IDWT), respectively. Here, the DWT decomposes x_e^k into four subbands $\{LL, LH, HL, HH\}$, and $F_d^k(\cdot)$ selectively suppresses redundant components in the wavelet domain while maintaining the reconstruction structure. Because x_d^{k+1} and the LL subband of $W(x_e^k)$ share the same spatial resolution, they can be directly fused via summation or concatenation, denoted by \oplus .

When the decoder transformation is omitted (i.e., $F_d^k(\cdot) = 0$), Eq. (3) reduces to:

$$x_d^k = W^\top W(x_e^k) = x_e^k, \quad (4)$$

indicating distortion-free reconstruction consistent

with the perfect reconstruction (PR) condition.

Formally, each SUPER block satisfies the suppressed reconstruction property

$$\Psi_k \Phi_k = I - \mathcal{S}_k, \quad |\mathcal{S}_k| \leq \epsilon, \quad (5)$$

where Φ_k and Ψ_k denote the encoder and decoder frame operators at stage k , and \mathcal{S}_k represents the learnable selective suppression in the wavelet domain. Thus, SUPER generalizes DCF’s reconstruction-aware stability into a plug-and-play decoder block that flexibly operates within modern encoder-decoder architectures.

4.2. Modular Design of SUPER

To facilitate practical integration, the proposed SUPER is modularized into a stage-wise algorithm that can serve as a plug-and-play component within diverse encoder-decoder architectures. At each decoder stage k , the block receives the skip feature x_e^k from the encoder and the output x_d^{k+1} from the deeper stage, maps them into the wavelet domain via $W(\cdot)$, and reconstructs the result through the inverse transform $W^\top(\cdot)$ after applying the selective decoder transformation $F_d^k(\cdot)$. The decoder transformation is fully architecture-agnostic and can include any convolutional, residual, or attention-based operation without frame constraints.

Feature Fusion. We fuse the encoder skip feature and decoder output either by summation or concatenation. For channel mismatch, a lightweight projection is applied only when necessary. When spatial resolutions differ, we avoid upsampling by adding the projected skip feature to the LL subband of the decomposed decoder feature, preserving alias-free fusion. This simple formulation maintains reconstruction fidelity while keeping the block compatible across diverse encoder-decoder architectures.

Implementation. Algorithm 1 summarizes this process,

abstracting away implementation-specific details such as convolution, normalization, or attention. Implementation details of the default blocks used in our experiments are provided in Appendix A, and reference code is available at our GitHub repository.

Algorithm 1. SUPER Decoder Block (stage k)

Inputs:

x_e^k : skip feature from encoder stage k, $[B, C^k, H, W]$
 x_d^{k+1} : output from k+1 stage, $[B, C^{k+1}, H/2, W/2]$
 F_d^k : generalized decoder block

Decoder^k_{SUPER}(x_e^k, x_d^{k+1}, F_d^k):

1. $\text{bands} \leftarrow \text{DWT}(e) // [B, 4C^k, H/2, W/2]$
2. $x \leftarrow \text{fusion}(\text{bands}, d) // \text{concat or sum}$
3. $\text{res} \leftarrow \text{CBAM}(F_d^k(x)) // [B, 4C^k, H/2, W/2]$
4. $\text{out} \leftarrow \text{IDWT}(\text{bands} - \text{chunk}(\text{res}))$

Outputs:

x_d^k : output from decoder stage k, $[B, C^k, H, W]$

total number of multiply–accumulate operations satisfies
 $MACs(H, W, C) \approx MACs(H/2, W/2, 4C)$.

Crucially, MAC differences across models originate from the layers applied after DWT, not from the transform. When subsequent convolutions operate on the 4C channels, the MACs reflect those architectural choices. In contrast, many upsampling-based decoders double spatial resolution while keeping channels fixed, causing their convolutional MACs to increase by approximately fourfold. The newly created pixels rely on interpolation, which introduces pseudo high-frequency artifacts lacking semantic meaning [31], [32], [33]. To compensate for these distortions and the increased spatial cost, such decoders often perform aggressive channel reduction, making their reported MACs lower—but at the expense of representational fidelity.

SUPER avoids this redundant spatial expansion and therefore does not require lossy channel compression. As a result, its MAC profile primarily reflects the intrinsic MAC-neutral property of the wavelet transform. Any remaining MAC differences arise from intentional architectural decisions, such as preserving the richer wavelet-decomposed representation, rather than from the transform itself.

Reconstruction-Aware Design. Because SUPER Decoder Block fuses multi-scale features entirely within the low-frequency (LL) band, the Nyquist frequency of the lower-resolution featured matches the LL bandwidth of the higher-resolution feature x_e^k . This physically consistent fusion avoids generating pseudo-high-frequency components, ensuring distortion-free, reconstruction-aware decoding without lossy compression.

5. Experimental Results

To verify the generality and structural robustness of the proposed SUPER Decoder Block, we design experiments across two spectrally complementary tasks: **thin-crack segmentation** (Sec. 5.1) and **smartphone image denoising** (Sec. 5.2). These tasks occupy opposite ends of the frequency spectrum—one dominated by fine, high-frequency structures and the other by smooth, low-frequency components—providing a complete spectrum-level validation.

Although both employ skip-connected encoder-decoder architectures, they differ fundamentally: **FACSN-Net** [24] integrates a hybrid convolution–transformer encoder with frequency-aware decoding, while **CascadedGaze-Net** [29] adopts a cascaded CNN framework emphasizing global context. Their structural diversity confirms that improvements arise from the reconstruction-aware design, not architectural coincidence.

All experiments use official SOTA implementations with identical optimization settings and hyperparameters; SUPER is inserted only into the decoder to ensure fair, structure-isolated comparison. Hardware details, software environments, pretrained weights, and

4.3. Design Advantages

Frequency-Aware Design. Deep neural networks suffer from **spectral bias**[10], [11], [22], preferring low-frequency components and thus losing fine details. Prior studies have commonly attempted to alleviate this issue through frequency-branch or frequency-aware designs [38], [39], which explicitly separate feature representations across spectral bands.

The SUPER Decoder Block inherently supports such frequency-divided processing through wavelet-domain decomposition, naturally providing subband-wise representation without requiring architectural branching. Moreover, high-frequency components are embedded within a lower Nyquist space, allowing them to be represented at reduced effective frequencies—thereby mitigating spectral bias while maintaining stable, alias-free detail representation [40].

Since wavelet subbands are interdependent, fully separate operations may break cross-band consistency. We first concatenate the subbands along the channel dimension, and apply CBAM [41] as a lightweight frequency-aware attention module that sequentially infers channel and spatial importance across subbands, thereby preserving cross-band consistency.

Overall, the SUPER Decoder Block achieves detail-sensitive yet spectrally consistent decoding, structurally mitigating spectral bias and further enhancing frequency selectivity through lightweight frequency attention, effectively addressing the low-frequency dominance inherent in conventional decoders.

Computational Analysis. A key point is that using a wavelet transform does not increase MACs [42]. DWT reduces spatial resolution by a factor of two in each dimension, and although it produces four subbands, the

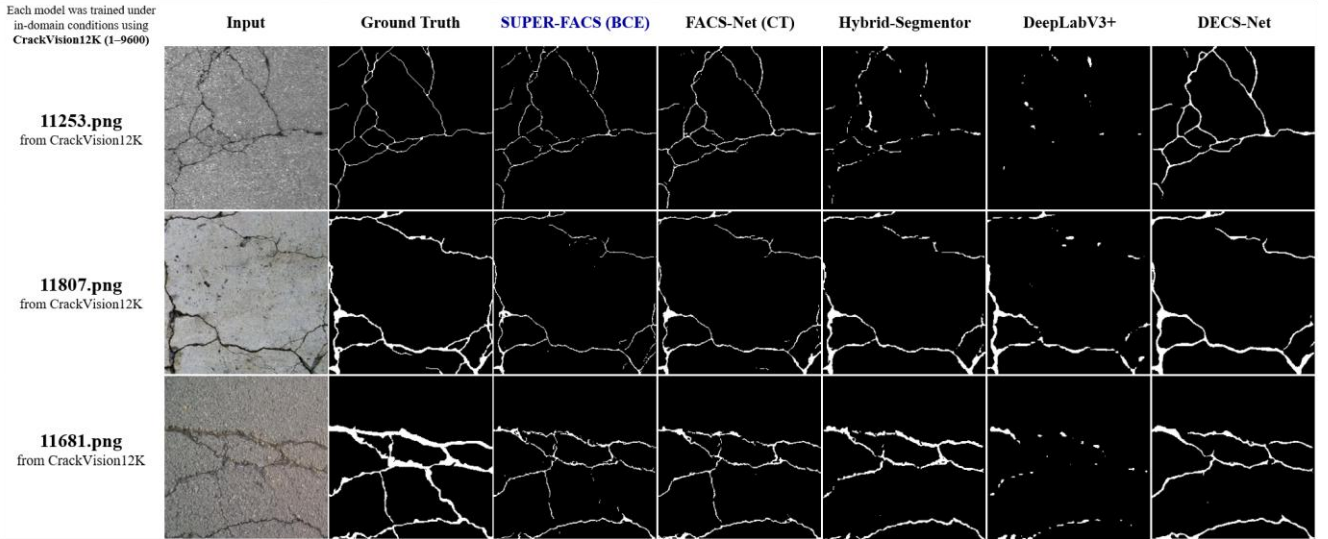


Figure 3. Qualitative Comparisons of Thin Crack Segmentation. Visual results for cracks thinner than 4 px, where prior methods show severe degradation.

qualitative results are provided in Appendix A for full reproducibility.

5.1. Evaluation on High-Frequency-Dominant Task: Thin-Crack Segmentation

Thin-crack segmentation critically depends on a network’s sensitivity to high-frequency structures. Minor distortions in fine edge reconstruction can cause substantial performance degradation even when global accuracy remains stable. The CrackVision12K dataset [43] provides an in-domain benchmark well-suited for assessing such sensitivity, as it includes crack annotations categorized by width. In prior work, FACS-Net [24]—a hybrid U-Net variant integrating convolution-transformer encoders and frequency-aware decoding—achieved state-of-the-art performance, particularly by addressing the severe accuracy drop observed for cracks thinner than 4 px in earlier benchmarks. Although extensive training data may improve robustness, this controlled in-domain setup remains the most effective for quantifying a model’s response to high-frequency detail.

In this section, we evaluate whether the proposed SUPER Decoder Block improves high-frequency reconstruction while preserving spectral consistency.

Implementation on FACS-Net. FACS-Net employs a hybrid encoder combining ResNet-50 [44] and Mix Transformer (MiT) [45], and a decoder composed of Double Convolution (DC) blocks [4] with resolution- and frequency-aware attention [37], [41].

To integrate the SUPER Decoder Block, we **augment** each decoder stage of FACS-Net with the SUPER blocks, where each F_d^k employs DC blocks, **and the original attention layers are omitted since SUPER already includes CBAM for subband-wise adaptive weighting**. The encoder remains unchanged; the resulting model is denoted **SUPER-FACS**.

Results on Thin Crack Segmentation. Quantitative

comparisons on CrackVision12K are summarized in Table 1, and qualitative examples of thin-crack reconstruction are shown in Figure 3.

For a fair and stable comparison, we thus report results using only the standard Binary Cross-Entropy (BCE) loss.

Even without any task-specific loss tuning, SUPER-FACS substantially outperformed the baseline FACS-Net trained with BCE, achieving higher IoU and Crack Topology Score (CTS) [46] values.

Importantly, both IoU and Crack Topology Score (CTS) recorded the highest values among all BCE-based models.

Ablation Results. For the ablation study, removing either CBAM or Selective Suppression (SS) from the SUPER decoder resulted in gradient vanishing in all ten runs, and training did not converge.

5.2. Evaluation on Low-Frequency-Dominant Task: Smartphone Image Denoising

Smartphone image denoising is a low-frequency-dominated problem because the ground-truth images in the SIDD [47], [48] are generated by multi-frame averaging, which inherently suppresses fine high-frequency details [49], [50]. As a result, most informative variations lie in the low-frequency domain, and performance depends largely on the model’s ability to preserve global luminance and structural consistency rather than local textures.

CascadedGaze-Net (CG-Net) [29] represents the state-of-the-art under this setting. Despite being fully CNN-based, its cascaded design efficiently aggregates global context through the Global Context Extraction (GCE) and NAF-based decoding blocks, achieving strong low-frequency reconstruction at minimal cost.

Such characteristics make this benchmark challenging for the proposed SUPER Decoder Block, since frequency-aware decoders tend to overemphasize high-frequency features, potentially weakening global smoothness and structural coherence [10], [22], [51].

Loss	Method	Metric	0–2	2–4	Average
Binary Cross Entropy (BCE-Loss)	SUPER-FACS	IoU	0.451	0.415	0.646
		CTS	0.916	0.806	0.593
	FACS-Net [24]	IoU	0.356	0.398	0.629
		CTS	0.872	0.778	0.532
	Hybrid-Segmentor [43] (BCE+Dice)	IoU	0.16	0.365	0.625
		CTS	0.585	0.819	0.619
	DeepLabV3+ [53]	IoU	0.079	0.301	0.595
		CTS	0.101	0.809	0.490
	DECS-Net [54]	IoU	0.275	0.301	0.564
		CTS	0.896	0.809	0.626

Table 1. Quantitative results on CrackVision12K Dataset. IoU and Crack Topology Score (CTS) for cracks of 0–2 px, 2–4 px, and overall average. The < 4 px range highlights the failure regime reported in prior work. SUPER-FACS (BCE only) outperforms BCE-trained FACS-Net.

Implementation on CG-Net. CG-Net consists of a GCE-block-based encoder and a NAF-block-based decoder [52]. When integrating the SUPER Decoder Block, the encoder remains unchanged, while each decoder stage replaces the original NAF block with a SUPER block using F_d^k constructed from NAF blocks. This model is referred to as **SUPER-CG**.

Results on Smartphone Image Denoising. Quantitative comparisons are summarized in Table 2.

SUPER-CG achieves the highest PSNR among all compared models while maintaining competitive SSIM, demonstrating clear improvement over the original CG-Net. Importantly, this gain is obtained without any denoising-specific loss engineering or task-specific architectural tuning.

6. Discussion

The experiments verify that the proposed SUPER Decoder Block can be seamlessly integrated into complex U-Net variants, confirming its role as a plug-and-play, reconstruction-aware decoder. Beyond performance gains, SUPER consistently demonstrates the structural benefits of frequency- and reconstruction-aware design, operating stably under unmodified SOTA settings.

Specifically, thin-crack segmentation and smartphone image denoising respectively probe the high-frequency sensitivity and low-frequency robustness of the model—two complementary extremes where conventional U-Net decoder variants typically fail to balance. SUPER’s consistent improvement across both validates its spectral generality and architecture-agnostic adaptability.

The following discussion analyzes these results from four perspectives: (1) enhanced high-frequency detail restoration, (2) robustness in low-frequency reconstruction, (3) structural stability and generality, and (4) current limitations and potential extensions.

6.1. High-Frequency Sensitivity

The thin-crack segmentation benchmark directly probes a model’s ability to retain fine, high-frequency

Method	PSNR \uparrow	SSIM \uparrow
SUPER-CG	40.416	0.964
CascadedGaze [29]	40.39	0.964
NAFNet [52]	40.30	0.962
Restormer [55]	40.02	0.960
CAT [56]	40.05	0.960
MAXIM [57]	39.96	0.958
HINet [58]	39.99	0.960
CycleISP [59]	39.52	0.957
MPRNet [60]	39.17	0.958

Table 2. Quantitative results on SIDD. Comparison of SUPER-CG with recent state-of-the-art denoising models.

structures and therefore serves as an effective test for reconstruction-aware decoding. Non-frequency-aware baselines, DeepLabV3+ and Hybrid-Segmentor, exhibit noticeable degradation on sub-4 px cracks, largely failing to localize thin boundaries—consistent with the known spectral bias of conventional decoders. Frequency-aware designs such as DECS-Net and FACS-Net recover most fine structures; however, DECS-Net tends to over-spread predictions, resulting in high CTS but lower IoU, while FACS-Net provides a more balanced reconstruction profile.

SUPER-FACS, trained solely with BCE, achieves the highest IoU and CTS among BCE-based models. This indicates that the proposed reconstruction-aware architecture inherently enhances high-frequency fidelity even without task-specific spectral regularization.

We also attempted to combine SUPER with CT-Loss. Because CT-Loss was originally tuned for the canonical FACS-Net decoder and relies on decoder-specific activation distributions, applying it to the SUPER-based variant required additional retuning and thus did not yield stable optimization under the default hyperparameters. As this behavior is tied to loss-architecture compatibility rather than the SUPER block itself, we report BCE-based comparisons for fair structural evaluation. A deeper loss-tuning study is left for future work.

6.2. Low-Frequency Robustness

Unlike segmentation, image denoising emphasizes stability in the low-frequency domain. Models focusing on high-frequency recovery often suffer PSNR degradation due to amplified gradients that destabilize global reconstruction [10], [22], [51].

SUPER-CG, however, maintains stable low-frequency behavior while surpassing CG-Net in PSNR. This suggests that the proposed reconstruction-aware structure provides a balanced spectral response—preserving detail fidelity without compromising large-scale coherence. Even when applied to a task where high-frequency cues are less dominant, SUPER consistently reinforces structural alignment and reduces distortions in the reconstructed signal.

Overall, the SIDD results highlight SUPER’s

robustness in low-frequency reconstruction and confirm its effectiveness as a spectrally balanced decoder across tasks with differing spectral emphases.

6.3. Structural Stability and Generality

Both FACS-Net and CG-Net represent highly evolved U-Net variants with distinct architectural philosophies. Yet, SUPER was seamlessly integrated into both without modifying encoders or training protocols, showing stable convergence and consistent performance gain.

Ablation studies further confirm that each subcomponent of SUPER contributes to this stability: removing either the spectral separation (SS) or CBAM leads to unstable gradients and degraded reconstruction. This indicates that the proposed design is not merely an add-on for performance, but a structurally coherent unit that regularizes decoder behavior.

These results demonstrate that SUPER serves as a universal, plug-and-play enhancement applicable across heterogeneous encoder-decoder architectures while preserving training stability.

6.4. Limitations and Future Directions

Despite its strong empirical performance, the current implementation of SUPER remains an early prototype. The block has so far been tested only on a Haar basis and within a limited set of U-Net variants, leaving more diverse evaluations and failure case analyses for future work. While the overall MACs remain unchanged, parameter growth slightly increases representational capacity, which may lead to overfitting without proper regularization.

These limitations suggest promising directions rather than structural weaknesses: exploring adaptive wavelet bases, frequency-selective regularization, and stability-aware optimization could further enhance generalization. Future work may also explore lightweight configurations for efficiency-critical tasks.

In summary, SUPER Decoder Block’s current scope demonstrates structural validity, and its identified limitations naturally point toward the next phase of refinement and generalization.

7. Conclusion

The SUPER framework reveals an architectural compatibility that has been missing in encoder-decoder design: while conventional U-Net decoders lack principled reconstruction capacity and wavelet-based decoders cannot benefit from modern pretrained encoders, SUPER enables their integration by providing a reconstruction module that is independent of encoder architecture. This bridges high-capacity transformers with wavelet-style decoders for the first time, offering a unified reconstruction pathway that preserves theoretical structure without constraining the choice of backbone.

Although our prototype is evaluated on only two spectrally extreme tasks, its consistent performance

across both high-frequency-sensitive and low-frequency-dominant settings indicates strong potential for broader applicability. Future research may extend SUPER with task-adaptive suppression, band-dependent decoder designs, and loss- or architecture-specific optimizations, positioning SUPER as a flexible reconstruction principle rather than a fixed block, and opening a wide space for next-generation frequency-aware decoder architectures.

References

- [1] A. A. Baniya, T.-K. Lee, P. Eklund, and S. Aryal, “A Survey of Deep Learning Video Super-Resolution,” *IEEE Trans. Emerg. Top. Comput. Intell.*, vol. 8, no. 4, pp. 2655–2676, Aug. 2024, doi: 10.1109/TETCI.2024.3398015.
- [2] A. Dede *et al.*, “Deep learning for efficient high-resolution image processing: A systematic review,” *Intell. Syst. Appl.*, vol. 26, p. 200505, June 2025, doi: 10.1016/j.iswa.2025.200505.
- [3] J. C. Ye, Y. Han, and E. Cha, “Deep Convolutional Framelets: A General Deep Learning Framework for Inverse Problems,” *SIAM J. Imaging Sci.*, vol. 11, no. 2, pp. 991–1048, Jan. 2018, doi: 10.1137/17M1141771.
- [4] O. Ronneberger, P. Fischer, and T. Brox, “U-Net: Convolutional Networks for Biomedical Image Segmentation,” May 18, 2015, *arXiv*: arXiv:1505.04597. doi: 10.48550/arXiv.1505.04597.
- [5] W. Jiangtao, N. I. R. Ruhaiyem, and F. Panpan, “A Comprehensive Review of U-Net and Its Variants: Advances and Applications in Medical Image Segmentation,” *IET Image Process.*, vol. 19, no. 1, p. e70019, 2025, doi: 10.1049/ipr2.70019.
- [6] P. Liu, H. Zhang, K. Zhang, L. Lin, and W. Zuo, “Multi-level Wavelet-CNN for Image Restoration,” May 22, 2018, *arXiv*: arXiv:1805.07071. doi: 10.48550/arXiv.1805.07071.
- [7] F. Zhang, S. B. Rangrej, T. Aumentado-Armstrong, A. Fazly, and A. Levinstein, “Augmenting Perceptual Super-Resolution via Image Quality Predictors”.
- [8] C. Zhang, X. Deng, and S. H. Ling, “Next-Gen Medical Imaging: U-Net Evolution and the Rise of Transformers,” *Sensors*, vol. 24, no. 14, p. 4668, July 2024, doi: 10.3390/s24144668.
- [9] X. Lin, Y. Li, J. Hsiao, C. Ho, and Y. Kong, “Catch Missing Details: Image Reconstruction with Frequency Augmented Variational Autoencoder,” in *2023 IEEE/CVF Conference on Computer Vision and Pattern Recognition (CVPR)*, Vancouver, BC, Canada: IEEE, June 2023, pp. 1736–1745. doi: 10.1109/CVPR52729.2023.00173.
- [10] N. Rahaman *et al.*, “On the Spectral Bias of Neural Networks,” in *Proceedings of the 36th International Conference on Machine Learning*, PMLR, May 2019, pp. 5301–5310. Accessed: Mar. 04, 2025. [Online]. Available: <https://proceedings.mlr.press/v97/rahaman19a.html>
- [11] Y. Cao, Z. Fang, Y. Wu, D.-X. Zhou, and Q. Gu, “Towards Understanding the Spectral Bias of Deep Learning,” Oct. 05, 2020, *arXiv*: arXiv:1912.01198. doi: 10.48550/arXiv.1912.01198.
- [12] H.-H. Yang and Y. Fu, “Wavelet U-Net and the Chromatic Adaptation Transform for Single Image Dehazing,” in *2019 IEEE International Conference on Image Processing (ICIP)*, Sept. 2019, pp. 2736–2740. doi: 10.1109/ICIP.2019.8803391.
- [13] X. Deng, R. Yang, M. Xu, and P. L. Dragotti, “Wavelet Domain Style Transfer for an Effective Perception-Distortion Tradeoff in Single Image Super-Resolution,” in *2019 IEEE/CVF International Conference on Computer Vision (ICCV)*, Seoul, Korea (South): IEEE, Oct. 2019, pp. 3076–3085. doi: 10.1109/ICCV.2019.00317.
- [14] R. Fang and Y. Xu, “Addressing Spectral Bias of Deep Neural Networks by Multi-Grade Deep Learning”.
- [15] Y. Zhao, S. Wang, Y. Zhang, S. Qiao, and M. Zhang, “WRANet: wavelet integrated residual attention U-Net network for medical image segmentation,” *Complex Intell. Syst.*, vol. 9, no. 6, pp. 6971–6983, Dec. 2023, doi: 10.1007/s40747-023-01119-y.
- [16] S. Akila Agnes, A. Arun Solomon, and K. Karthick, “Wavelet U-Net++ for accurate lung nodule segmentation in CT scans: Improving early detection and diagnosis of lung cancer,” *Biomed. Signal Process. Control*, vol. 87, p. 105509, Jan. 2024, doi: 10.1016/j.bspc.2023.105509.
- [17] E. Marcus, R. Sheombarsing, J.-J. Sonke, and J. Teuwen, “Task-Driven Wavelets Using Constrained Empirical Risk Minimization,” in *2024 IEEE/CVF Conference on Computer Vision and Pattern Recognition (CVPR)*, Seattle, WA, USA: IEEE, June 2024, pp. 24098–24107. doi: 10.1109/CVPR52733.2024.02275.
- [18] L. Jiang, B. Dai, W. Wu, and C. C. Loy, “Focal Frequency Loss for Image Reconstruction and Synthesis,” in *2021 IEEE/CVF International Conference on Computer Vision (ICCV)*, Montreal, QC, Canada: IEEE, Oct. 2021, pp. 13899–13909. doi: 10.1109/ICCV48922.2021.01366.
- [19] W. Yang *et al.*, “Optimizing transformer-based network via advanced decoder design for medical image segmentation,” *Biomed. Phys. Eng. Express*, vol. 11, no. 2, p. 025024, Mar. 2025, doi: 10.1088/2057-1976/adaec7.
- [20] J. C. Santos, H. Tomás Pereira Alexandre, M. Seoane Santos, and P. Henriques Abreu, “The Role of Deep Learning in Medical Image Inpainting: A Systematic Review,” *ACM Trans. Comput. Healthc.*, vol. 6, no. 3, pp. 1–24, July 2025, doi: 10.1145/3712710.
- [21] B. Yu, Q. Zhou, L. Yuan, H. Liang, P. Shcherbakov, and X. Zhang, “3D medical image segmentation using the serial-parallel convolutional neural network and transformer based on cross-window self-attention,” *CAAI Trans. Intell. Technol.*, vol. 10, no. 2, pp. 337–348, Apr. 2025, doi: 10.1049/cit2.12411.
- [22] Z.-Q. J. Xu, L. Zhang, and W. Cai, “On understanding and overcoming spectral biases of deep neural network learning methods for solving PDEs,” Jan. 17, 2025, *arXiv*: arXiv:2501.09987. doi: 10.48550/arXiv.2501.09987.

[23] Y. Wu, S. Li, J. Li, Y. Yu, J. Li, and Y. Li, “Deep learning in crack detection: A comprehensive scientometric review,” *J. Infrastruct. Intell. Resil.*, vol. 4, no. 3, p. 100144, Sept. 2025, doi: 10.1016/j.iintel.2025.100144.

[24] S. Joo, S. Kim, and H. Kim, “Frequency-Aware Crack Segmentation Network (FACS-Net) for Thin-Cracks via Topology Preservation”.

[25] A. Zaman *et al.*, “Adaptive Feature Medical Segmentation Network: an adaptable deep learning paradigm for high-performance 3D brain lesion segmentation in medical imaging,” *Front. Neurosci.*, vol. 18, p. 1363930, Apr. 2024, doi: 10.3389/fnins.2024.1363930.

[26] J. Peng, M. Lu, B. Li, J. Wang, W. Hu, and X. Liu, “Frequency-aware denoising using a diffusion model for enhanced band-limited and white noise removal in x-ray acoustic computed tomography,” *Med. Phys.*, vol. 52, no. 5, pp. 3325–3335, May 2025, doi: 10.1002/mp.17681.

[27] N. Mu, Z. Lyu, X. Zhang, R. McBane, A. S. Pandey, and J. Jiang, “Exploring a Frequency-Domain Attention-Guided Cascade U-Net: Towards Spatially Tunable Segmentation of Vasculature,” *Comput. Biol. Med.*, vol. 167, p. 107648, Dec. 2023, doi: 10.1016/j.combiomed.2023.107648.

[28] S. Joo, S. Kim, and H. Kim, “Frequency-Aware Crack Segmentation Network (Facs-Net) for Thin-Cracks Via Topology Preservation,” Aug. 08, 2025, *Social Science Research Network, Rochester, NY*: 5384487. doi: 10.2139/ssrn.5384487.

[29] A. Ghasemabadi, M. K. Janjua, M. Salameh, C. Zhou, F. Sun, and D. Niu, “CascadedGaze: Efficiency in Global Context Extraction for Image Restoration,” May 07, 2024, *arXiv*: arXiv:2401.15235. doi: 10.48550/arXiv.2401.15235.

[30] O. T. Paalvast, O. Hertgers, M. Sevenster, and H. J. Lamb, “Assessing the Image Quality of Digitally Reconstructed Radiographs from Chest CT,” *J. Imaging Inform. Med.*, Jan. 2025, doi: 10.1007/s10278-025-01406-9.

[31] I. Aganj, B. T. T. Yeo, M. R. Sabuncu, and B. Fischl, “On Removing Interpolation and Resampling Artifacts in Rigid Image Registration,” *IEEE Trans. Image Process.*, vol. 22, no. 2, pp. 816–827, Feb. 2013, doi: 10.1109/TIP.2012.2224356.

[32] A. H. Ribeiro and T. B. Schön, “How Convolutional Neural Networks Deal with Aliasing,” Feb. 15, 2021, *arXiv*: arXiv:2102.07757. doi: 10.48550/arXiv.2102.07757.

[33] C. Tan *et al.*, “Rethinking the Up-Sampling Operations in CNN-based Generative Network for Generalizable Deepfake Detection,” Dec. 20, 2023, *arXiv*: arXiv:2312.10461. doi: 10.48550/arXiv.2312.10461.

[34] X. Gou, C. Liao, J. Zhou, F. Ye, and Y. Lin, “FIF-UNet: An Efficient UNet Using Feature Interaction and Fusion for Medical Image Segmentation,” Sept. 09, 2024, *arXiv*: arXiv:2409.05324. doi: 10.48550/arXiv.2409.05324.

[35] S. Sawant, A. Medgyesy, S. Raghunandan, and T. Götz, “LMSC-UNet: A Lightweight U-Net with Modified Skip Connections for Semantic Segmentation;,” in *Proceedings of the 17th International Conference on Agents and Artificial Intelligence*, Porto, Portugal: SCITEPRESS - Science and Technology Publications, 2025, pp. 726–734. doi: 10.5220/0013343800003890.

[36] J. Zeng, L. Huang, and K. Wang, “WST: Wavelet-Based Multi-scale Tuning for Visual Transfer Learning”.

[37] Q. Bu, D. Huang, and H. Cui, “Towards Building More Robust Models with Frequency Bias,” in *2023 IEEE/CVF International Conference on Computer Vision (ICCV)*, Paris, France: IEEE, Oct. 2023, pp. 4379–4388. doi: 10.1109/ICCV51070.2023.00406.

[38] M. Tancik *et al.*, “Fourier Features Let Networks Learn High Frequency Functions in Low Dimensional Domains,” in *Advances in Neural Information Processing Systems*, Curran Associates, Inc., 2020, pp. 7537–7547. Accessed: Oct. 10, 2025. [Online]. Available: https://papers.neurips.cc/paper_files/paper/2020/hash/h55053683268957697aa39fba6f231c68-Abstract.html

[39] Z. Li *et al.*, “Fourier Neural Operator for Parametric Partial Differential Equations,” May 17, 2021, *arXiv*: arXiv:2010.08895. doi: 10.48550/arXiv.2010.08895.

[40] V. Sitzmann, J. Martel, A. Bergman, D. Lindell, and G. Wetzstein, “Implicit Neural Representations with Periodic Activation Functions,” in *Advances in Neural Information Processing Systems*, Curran Associates, Inc., 2020, pp. 7462–7473. Accessed: Oct. 10, 2025. [Online]. Available: <https://proceedings.neurips.cc/paper/2020/hash/53c04118df112c13a8c34b38343b9c10-Abstract.html>

[41] S. Woo, J. Park, J.-Y. Lee, and I. S. Kweon, “CBAM: Convolutional Block Attention Module,” in *Computer Vision – ECCV 2018*, vol. 11211, V. Ferrari, M. Hebert, C. Sminchisescu, and Y. Weiss, Eds., in *Lecture Notes in Computer Science*, vol. 11211., Cham: Springer International Publishing, 2018, pp. 3–19. doi: 10.1007/978-3-030-01234-2_1.

[42] Y. Zhang *et al.*, “Model-based Analysis of ChIP-Seq (MACS),” *Genome Biol.*, vol. 9, no. 9, p. R137, Sept. 2008, doi: 10.1186/gb-2008-9-9-r137.

[43] J. M. Goo, X. Milidonis, A. Artusi, J. Boehm, and C. Ciliberto, “Hybrid-Segmentor: Hybrid approach for automated fine-grained crack segmentation in civil infrastructure,” *Autom. Constr.*, vol. 170, p. 105960, Feb. 2025, doi: 10.1016/j.autcon.2024.105960.

[44] K. He, X. Zhang, S. Ren, and J. Sun, “Deep Residual Learning for Image Recognition,” in *2016*

IEEE Conference on Computer Vision and Pattern Recognition (CVPR), Las Vegas, NV, USA: IEEE, June 2016, pp. 770–778. doi: 10.1109/CVPR.2016.90.

[45] E. Xie, W. Wang, Z. Yu, A. Anandkumar, J. M. Alvarez, and P. Luo, “SegFormer: Simple and Efficient Design for Semantic Segmentation with Transformers,” Oct. 28, 2021, *arXiv*: arXiv:2105.15203. doi: 10.48550/arXiv.2105.15203.

[46] J. Hyeon, M. Jeong, W.-C. Chern, V. K. Asari, and H. Kim, “Evaluating Road Crack Segmentation Performance in Participatory Sensing: An Exploration of Alternative Metrics,” *J. Comput. Civ. Eng.*, vol. 39, no. 5, p. 04025064, Sept. 2025, doi: 10.1061/JCCEE5.CPENG-6011.

[47] A. Abdelhamed, S. Lin, and M. S. Brown, “A High-Quality Denoising Dataset for Smartphone Cameras,” in *2018 IEEE/CVF Conference on Computer Vision and Pattern Recognition*, Salt Lake City, UT: IEEE, June 2018, pp. 1692–1700. doi: 10.1109/CVPR.2018.00182.

[48] A. Abdelhamed *et al.*, “NTIRE 2019 Challenge on Real Image Denoising: Methods and Results,” in *2019 IEEE/CVF Conference on Computer Vision and Pattern Recognition Workshops (CVPRW)*, Long Beach, CA, USA: IEEE, June 2019, pp. 2197–2210. doi: 10.1109/CVPRW.2019.00273.

[49] T. Plotz and S. Roth, “Benchmarking Denoising Algorithms with Real Photographs,” in *2017 IEEE Conference on Computer Vision and Pattern Recognition (CVPR)*, Honolulu, HI: IEEE, July 2017, pp. 2750–2759. doi: 10.1109/CVPR.2017.294.

[50] S. W. Zamir *et al.*, “Learning Enriched Features for Real Image Restoration and Enhancement,” in *Computer Vision – ECCV 2020*, vol. 12370, A. Vedaldi, H. Bischof, T. Brox, and J.-M. Frahm, Eds., in *Lecture Notes in Computer Science*, vol. 12370. , Cham: Springer International Publishing, 2020, pp. 492–511. doi: 10.1007/978-3-030-58595-2_30.

[51] R. Fang and Y. Xu, “Addressing Spectral Bias of Deep Neural Networks by Multi-Grade Deep Learning,” Oct. 21, 2024, *arXiv*: arXiv:2410.16105. doi: 10.48550/arXiv.2410.16105.

[52] L. Chen, X. Chu, X. Zhang, and J. Sun, “Simple Baselines for Image Restoration,” in *Computer Vision – ECCV 2022*, vol. 13667, S. Avidan, G. Brostow, M. Cissé, G. M. Farinella, and T. Hassner, Eds., in *Lecture Notes in Computer Science*, vol. 13667. , Cham: Springer Nature Switzerland, 2022, pp. 17–33. doi: 10.1007/978-3-031-20071-7_2.

[53] Z. Yu, C. Dai, X. Zeng, Y. Lv, and H. Li, “A lightweight semantic segmentation method for concrete bridge surface diseases based on improved DeeplabV3+,” *Sci. Rep.*, vol. 15, no. 1, p. 10348, Mar. 2025, doi: 10.1038/s41598-025-95518-5.

[54] J. Zhang, Z. Zeng, P. K. Sharma, O. Alfarraj, A. Tolba, and J. Wang, “A dual encoder crack segmentation network with Haar wavelet-based high–low frequency attention,” *Expert Syst. Appl.*, vol. 256, p. 124950, Dec. 2024, doi: 10.1016/j.eswa.2024.124950.

[55] S. W. Zamir, A. Arora, S. Khan, M. Hayat, F. S. Khan, and M.-H. Yang, “Restormer: Efficient Transformer for High-Resolution Image Restoration,” in *2022 IEEE/CVF Conference on Computer Vision and Pattern Recognition (CVPR)*, New Orleans, LA, USA: IEEE, June 2022, pp. 5718–5729. doi: 10.1109/CVPR52688.2022.00564.

[56] Z. Chen, Y. Zhang, J. Gu, Y. Zhang, L. Kong, and X. Yuan, “Cross Aggregation Transformer for Image Restoration”.

[57] Z. Tu *et al.*, “MAXIM: Multi-Axis MLP for Image Processing,” in *2022 IEEE/CVF Conference on Computer Vision and Pattern Recognition (CVPR)*, New Orleans, LA, USA: IEEE, June 2022, pp. 5759–5770. doi: 10.1109/CVPR52688.2022.00568.

[58] L. Chen, X. Lu, J. Zhang, X. Chu, and C. Chen, “HINet: Half Instance Normalization Network for Image Restoration,” in *2021 IEEE/CVF Conference on Computer Vision and Pattern Recognition Workshops (CVPRW)*, Nashville, TN, USA: IEEE, June 2021, pp. 182–192. doi: 10.1109/CVPRW53098.2021.00027.

[59] S. W. Zamir *et al.*, “CycleISP: Real Image Restoration via Improved Data Synthesis,” in *2020 IEEE/CVF Conference on Computer Vision and Pattern Recognition (CVPR)*, Seattle, WA, USA: IEEE, June 2020, pp. 2693–2702. doi: 10.1109/CVPR42600.2020.00277.

[60] S. W. Zamir *et al.*, “Multi-Stage Progressive Image Restoration,” in *2021 IEEE/CVF Conference on Computer Vision and Pattern Recognition (CVPR)*, Nashville, TN, USA: IEEE, June 2021, pp. 14816–14826. doi: 10.1109/CVPR46437.2021.01458.

Appendix A. Github Repository

This appendix will be released in a future update. We are preparing additional analyses, extended experiments, and implementation details to support the main paper. All supplementary materials will be made publicly available upon finalization.